This paper first appeared in the thirteenth print edition of the *Photovoltaics International* journal, published in August 2011.

High-efficiency rear-passivated screen-printed silicon solar cells

Thorsten Dullweber[1], **Sebastian Gatz**[1], **Tom Falcon**[2] & **Helge Hannebauer**[1]
[1] Institute for Solar Energy Research Hamelin (ISFH), Emmerthal, Germany; [2] DEK Printing Machines Ltd, Weymouth, UK

ABSTRACT

Approximately 80% of today's silicon solar cells industrially manufactured worldwide apply screen printing for the metallization of the silver front and aluminium rear contacts. In production, conversion efficiencies of ~18–18.5% are achieved using monocrystalline silicon wafers. A baseline process has been implemented at ISFH that is very similar to the industry-standard process, displaying conversion efficiencies of up to 18.5%. An analysis of the solar cells reveals that the conversion efficiency is limited in particular by the shadowing loss due to the silver front-side metallization, as well as infrared light being absorbed in the aluminium rear-side metallization. This paper summarizes recent developments at ISFH that resulted in a 19.4% efficient large-area screen-printed solar cell, when applying a print-on-print silver front-side metallization and an SiO_2/SiN_x rear-surface passivation.

Introduction

Today, about 80% of silicon solar cells industrially manufactured worldwide apply screen printing for the deposition of the silver front and the full-area aluminium rear metal contacts, as shown in the schematic drawing in Fig. 1a. In production, conversion efficiencies of ~18–18.5% are demonstrated on monocrystalline silicon wafers [1]. Among other factors, two loss mechanisms limit the conversion efficiency of these cells: 1) the silver front-side metallization with finger widths of ~90–100µm reflects about 7% of the incident solar radiation; and 2) the screen-printed full-area aluminium back-surface field (Al-BSF) exhibits only a moderate passivation quality, with typical rear-surface recombination velocities ($S_{eff,rear}$) ranging from 200 to 600cm/s [2,3]. In addition, only about 65% of the infrared light reaching the aluminium rear contact is reflected back into the silicon wafer [4].

To reduce the front-side shading loss, one promising approach is the print-on-print (PoP) technique, in which the silver front contact is deposited in two consecutive screen-printing steps, resulting in a smaller finger width with a higher aspect ratio and hence increased conversion efficiencies [5–7]. The electrical and optical losses of the full-area Al-BSF on the rear side can be reduced by PERC (passivated emitter and rear cell) solar cell design, which is shown in the

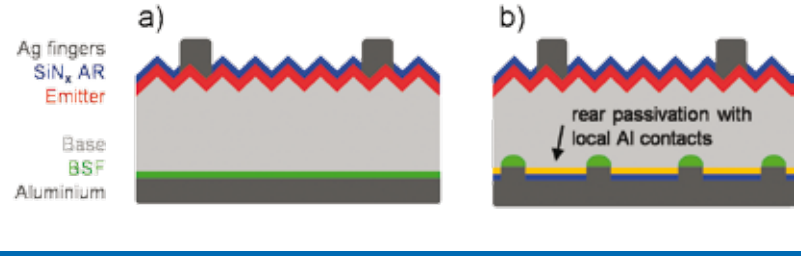

Figure 1. Schematic drawings of a) typical industrial screen-printed silicon solar cell with full-area Al-BSF, and b) PERC solar cell with dielectric rear passivation and screen-printed local aluminium contacts to the silicon base. The rear passivation layer typically consists of a passivation layer (yellow) and an SiN_x capping layer (blue).

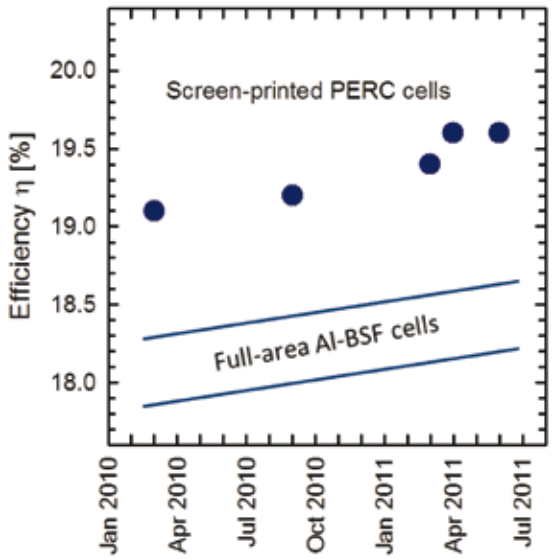

Figure 2. Recent record conversion efficiencies [14–19] of screen-printed rear-passivated PERC solar cells, applying large-area monocrystalline p-type silicon wafers. As a reference, typical conversion efficiencies [1] of industrially manufactured monocrystalline silicon solar cells, with a screen-printed full-area Al-BSF are also indicated.

schematic drawing in Fig. 1b. The PERC cell design has already been applied to laboratory-type silicon solar cells in 1989 [8]. At the rear of the cell, a significantly improved surface passivation and optical reflectance is achieved by dielectric layers, such as SiO_2 [9,10], SiN_x [9], SiC_x [11] and Al_2O_3 [12,13], compared to the full-area Al-BSF. Fig. 2 shows recent record conversion efficiencies for industrial-type (large-area wafers, screen-printed metallization) PERC *p*-type silicon solar cells, which improved from 19.1% in March 2010 to 19.6% in April 2011 [14–19].

This paper presents a summary of recent results demonstrated at ISFH for screen-printed rear-passivated PERC cells, with conversion efficiencies of up to 19.4% [16]. We describe our baseline process for screen-printed solar cells, provide details of the PoP silver front-side metallization and compare two different rear passivation layer stacks: SiO_2/SiN_x and Al_2O_3/SiN_x.

ISFH baseline process for screen-printed full-area Al-BSF silicon solar cells

At ISFH we have established a reference process for screen-printed silicon solar cells and consider it to be very similar to today's standard industrial processing sequence. Pseudo-square 125 × 125mm² 2–3Ωcm *p*-type boron-doped Cz-silicon wafers with a starting thickness of 200µm are used in this process. After applying a KOH/IPA-based wet chemical surface texture, the n^+-emitter is formed by $POCl_3$ diffusion with a sheet resistance R_{sheet} of 60 to 70Ω/sq. The phosphorus silicate glass is removed by an HF etch. The front side is coated with an SiN_x antireflective layer with a refractive index of 2.05 and a thickness of 70nm. Afterwards, the Ag front contacts are screen printed using a DEK PVP1200 printer, resulting in a finger width ~110µm (see Fig. 3b). The Al rear contact is full-area screen printed, and after each printing step, the pastes are dried in a belt furnace. The processing is completed by a co-firing step in a conveyor belt furnace, followed by the laser edge isolation.

The resulting standard screen-printed solar cells show conversion efficiencies η of up to 18.5%, as displayed in Table 1, cell A. On a larger number of identically processed standard screen-printed solar cells, the standard deviation of the conversion efficiency was determined to be ±0.1%. The small spread of the conversion efficiency allows statistically relevant experiments with a small number of solar cells, e.g. 5 or 10 cells, per split group.

PoP silver front-side metallization

We significantly reduce the silver finger width by applying and optimizing the PoP process. In this case, the Ag front contact is deposited in two consecutive screen-printing steps using a DEK PVP1200

Cell	Type	Rear side	Pitch [mm]	Finger width [µm]	η[%]	V_{oc} [mV]	J_{sc} [mA/cm²]	FF [%]	Rs [Ωcm²]
A	Ref.	Al-BSF	-	110	18.5	633	37.0	79.2	0.6
B_1	PoP	Al-BSF	-	70	18.9	634	37.4	79.7	0.6
B_2	PoP	Al-BSF	-	70	18.7*	632	37.1	79.8	0.6
C	PERC	Al_2O_3/SiN_x	1	90	19.0*	652	38.9	75.1	1.3
D	PERC	SiO_2/SiN_x	2	90	19.4*	664	38.5	75.8	1.6

* independently confirmed by FhG-ISE CalLab

Table 1. Solar cell parameters measured under standard testing conditions. Cell A refers to a standard screen-printed solar cell with a full-area Al-BSF and single-printed Ag front contacts. Cells B_1 and B_2 received a PoP Ag front-side metallization with reduced finger width. Cells C and D apply a rear-side passivation of Al_2O_3/SiN_x and SiO_2/SiN_x, respectively, in addition to the PoP Ag metallization.

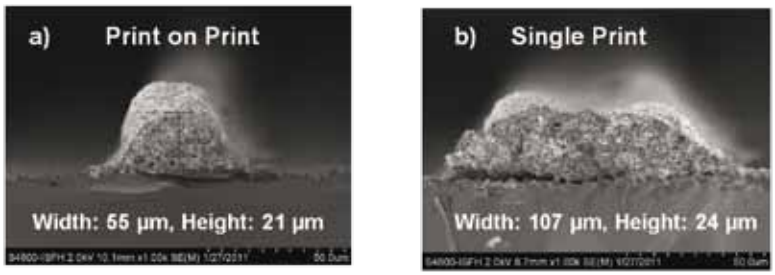

Figure 3. SEM cross-section images of silver front-contact fingers after firing on fully processed solar cells, applying a) PoP screen printing, with finger width 55µm and height 21µm, and b) standard single printing, with finger width 107µm and height 24µm.

printer. Both screens used in the two printing steps are mesh-type screens. In the first screen-printing step, an Ag paste Ag1 is applied, which is designed to establish a good contact resistance to the emitter. After drying, the second Ag screen-printing step follows, using an Ag paste Ag2 with low specific resistivity, in order to reduce the finger line resistance. The second print is completed again by a drying step. Both printing steps are highly accurately aligned towards the four edges of the silicon wafer by a vision camera system in the PVP1200 printer, which ensures ±12.5µm alignment accuracy at 6 sigma and hence an excellent alignment of the second print on the first print.

> "The PoP solar cells achieve conversion efficiencies of up to 18.9%."

The resulting PoP Ag finger profile after firing is shown in the scanning electron microscope (SEM) cross section in Fig. 3a. For comparison, a standard single-printed Ag finger is given in Fig. 3b. The PoP process reduces the finger width to 55µm while maintaining a similar finger height of 21µm. Optical-light microscope measurements reveal average finger widths of (70±5)µm (see cells B_1 and B_2 in Table 1). The smaller finger width reduces the shadowing loss from 6.7% for single print, to 5.4% for PoP with 70µm finger width.

The PoP solar cells achieve conversion efficiencies of up to 18.9% (see cells B_1 and B_2 in Table 1). The value of J_{sc} increases by 0.4mA/cm^2 to 37.4mA/cm^2, due to the reduced shadowing loss. In addition, the PoP cells show an excellent fill factor (FF) of up to 79.8% and a series resistance (R_s) of 0.6Ωcm^2, which indicates that there is no issue regarding contact resistance or line resistance. Besides increasing the conversion efficiency, PoP also reduces the amount of Ag paste deposited on a solar cell by approximately 20–25%, which is important due to the high costs of Ag pastes.

Numerical simulation of screen-printed PERC solar cells

In order to estimate the efficiency potential of industrial-type solar cells with dielectric rear passivation, PC1D simulations are carried out assuming typical input parameters derived from the analysis of our screen-printed solar cells, e.g. a front-side metallization shadowing loss of 6.7%, a 60Ω/sq emitter with a saturation current density of 230fA/cm^2 and a bulk minority carrier lifetime of 400µs. The rear-surface recombination velocity $S_{eff,rear}$ and the internal reflectance R_{rear} at the rear of the cell are varied; both of these strongly influence the efficiency as shown in Fig. 4. Whereas the full-area Al-BSF with $S_{eff,rear}$ = 400cm/s and R_{rear} = 65% limits the efficiency of typical industrial cells to ~18.5%, PERC cells with dielectric rear passivation have the potential to achieve efficiencies η > 19.5% if $S_{eff,rear}$ < 100cm/s and R_{rear} > 90%.

Process sequence of screen-printed PERC solar cells

Based on the process flow of the full-area Al-BSF solar cells described above, we have developed a process sequence that includes a passivation of the rear side of the cell by applying dielectric layer stacks. Full processing details are described in [16], but here only the most important process steps will be highlighted. Before texturing and phosphorus diffusion, a dielectric protection layer is deposited on the rear side of the solar cell, leaving the rear side planar and boron doped. Two different rear passivation layers are investigated: a 10nm plasma-assisted ALD-Al_2O_3 layer [20] and a 10nm thermal SiO_2 layer. The double-sided oxidation step for the PERC cells with SiO_2 passivation affects the n^+-emitter profile, leading to reduced emitter saturation currents [16,21]. A PECVD-SiN_x layer is deposited on top of the passivation layer at the rear to improve both the optical reflectance and the surface passivation quality. The dielectric layer stacks at the rear are locally ablated by laser contact opening (LCO) in order to form local line openings. The approximately 80µm-wide line openings are equidistantly spaced with a pitch of either 1mm or 2mm for cells C and D, respectively (see Table 1). Line openings are chosen instead of point

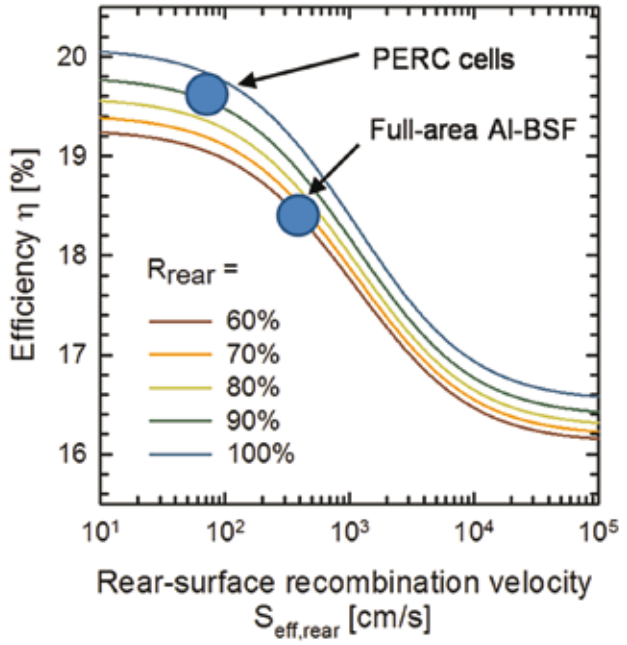

Figure 4. PC1D simulation of the conversion efficiency η vs. the rear-surface recombination velocity $S_{eff,rear}$ for different internal rear reflectance values R_{rear}. Whereas the full-area Al-BSF of typical industrial-type silicon solar cells with $S_{eff,rear}$ = 400cm/s and R_{rear} = 65% limits the conversion efficiency to ~18.5%, screen-printed PERC cells with dielectric rear passivation have the potential to achieve 20% conversion efficiency.

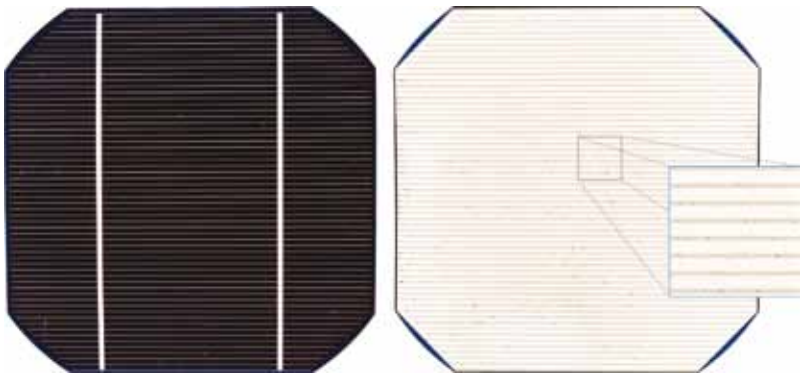

Figure 5. Photographs of the front and rear sides of a PERC solar cell with 19.4% conversion efficiency. Whereas the front side is very similar to a standard screen-printed solar cell, the rear side shows the dielectric passivation layer and the local line contacts.

contacts, since line openings facilitate the formation of a deep and uniform local Al-BSF [22].

The Ag front contacts are deposited by the same PoP screen-printing process as described in the previous section. However, for the rear-passivated cells, the Ag finger width is ~90µm instead of 70µm, which might be partly caused by the increased reflectance of the rear side of the wafer, reducing the wafer edge alignment accuracy of the PVP1200 printer. However, this is still subject to further analysis and optimization. The first PoP evaluations on PERC cells applying a DEK Eclipse printer show very promising results. The Al rear contact is formed by standard full-area Al screen printing. We apply an Al paste Al2, designed for local contacts for the PERC cells C and D, as compared to the standard paste Al1, used for the cells A and B in Table 1. In [23], we show that the paste Al2 achieves a deeper and more uniform local Al-BSF, resulting in significantly lower surface recombination velocities. The laser edge isolation is not required for PERC cells C and D, since only the front side is phosphorus doped. Fig. 5 shows photographs of the front and rear sides of the final cell. The contact lines on the rear side of the cell as well as the passivation layer are clearly visible.

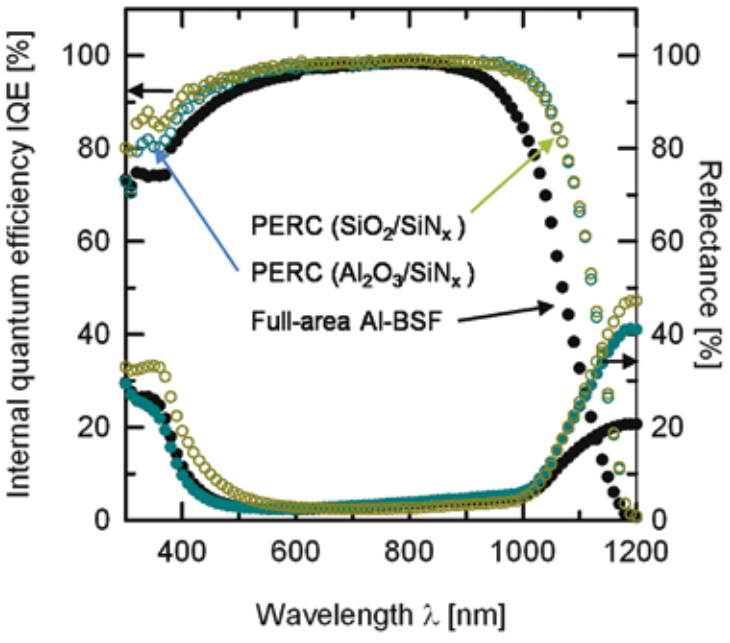

Figure 7. Comparison of IQE and reflectance between PERC solar cells with Al_2O_3/SiN_x (cell C in Table 1) and SiO_2/SiN_x (cell D) passivation stacks at the rear and a full-area Al-BSF reference cell (B_2).

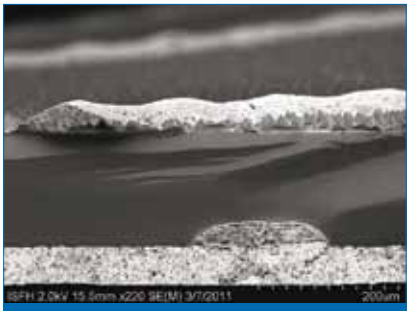

Figure 6. SEM cross-section image of a screen-printed, rear-side-passivated PERC solar cell with local line contacts on the rear side. Horizontal dimensions of the finger width and the line contact width deduced from this image have to be divided by √2, due to the 45-degree cross-section angle.

> "Screen-printed PERC cells with dielectric rear passivation have the potential to achieve 20% conversion efficiency."

The SEM cross section of the PERC solar cell in Fig. 6 shows the local Al contact at the rear, with a uniform Al-BSF above the Al-Si eutectic layer. The Ag finger is approximately 90µm wide, and the local Al contact has a width of approximately 140µm. (The cross section has been taken along the <110> crystallographic orientation at an angle of 45 degrees with respect to the Ag fingers and local line contacts at the rear. Accordingly, the horizontal dimensions of the finger width and the line contact width deduced from this image have to be divided by √2.)

IV and IQE analysis of screen-printed PERC cells

Table 1 shows the measured cell parameters of the PERC solar cells C and D with Al_2O_3/SiN_x and with SiO_2/SiN_x rear passivation stacks. The PERC cells are measured after deactivation of boron-oxygen-related recombination by simultaneously annealing for 6 hours at 140°C and illuminating with white light [24,25]. PERC solar cells C and D achieve independently confirmed conversion efficiencies of 19.0% and 19.4%, respectively. Both PERC solar cells show a noticeable improvement in J_{sc} of up to 38.9mA/cm^2. Moreover, the SiO_2/SiN_x-passivated PERC cell D shows a significantly improved open-circuit voltage V_{oc} of 664mV, which is attributable to the changed emitter profile as described

above. However, the FF of ~75% for the PERC solar cells is much lower compared to the FF of 79.8% for the reference cell B_2. The decreased FF is caused by a considerably increased series resistance from 0.6Ωcm² for the full Al-BSF reference cells, to 1.3Ωcm² and 1.6Ωcm² for the PERC cells C and D, respectively. The analysis and investigation [26] reveals that, in particular, a relatively high specific contact resistance of 55mΩcm² of the local screen-printed Al contacts is the cause of the marked increase in series resistance and hence the reduced FF. This is subject to further analysis and optimization.

The reflectance and internal quantum efficiency (IQE) of PERC and Al-BSF solar cells are shown in Fig. 7. In the long-wavelength region λ > 900nm, the dielectric rear-surface passivation significantly improves the reflectance and the IQE. With analytical modelling, we obtain $S_{eff,rear}$ = (70±30)cm/s for PERC cell C and $S_{eff,rear}$ = (80±30) cm/s for PERC cell D, compared to the full-area Al-BSF solar cell B_2 with $S_{eff,rear}$ of (350±100)cm/s. In the short-wavelength region λ < 500nm, the SiO_2/SiN_x-passivated PERC cell D shows the highest IQE, due to the changed emitter doping profile (R_{sheet} = 80Ω/sq), as compared to the Al_2O_3/SiN_x-passivated PERC cell (R_{sheet} = 70Ω/sq) and the full-area Al-BSF reference cell (R_{sheet} = 55Ω/sq).

The reduced surface recombination velocities at the rear contribute to the improvement in V_{oc} shown in Table 1 for the PERC cells. The increase in J_{sc} of up to 1.5mA/cm² is due to the excellent rear-surface passivation, combined with an improvement of the internal rear reflectance from 61% to 89% and 91%, respectively.

Conclusions and outlook

Based on a solar cell process that is very similar to today's industrially manufactured full-area Al-BSF screen-printed solar cells, we have shown that the PoP silver front-side metallization reduces the finger width to 70µm and minimizes the shadowing loss to 5.4%, which increases the conversion efficiency to 18.9%. The implementation of a dielectric rear passivation greatly reduces the rear-surface recombination velocity $S_{eff,rear}$ to 70cm/s for Al_2O_3/SiN_x and 80cm/s for SiO_2/SiN_x. Additionally, the dielectric layers significantly increase the internal reflectance to 91%, which results in independently confirmed increased conversion efficiencies to 19.4% for large-area silicon solar cells metallized by screen printing. The conversion efficiency is mainly limited by a relatively low fill factor of 75.8% due to a high specific contact resistance of ~55mΩcm² of the local Al contacts. Future improvements of the screen-printed local Al contact formation should enable conversion efficiencies close to 20%. The implementation of a selective emitter into the PERC cell, as well as a reduction of the Ag finger width to 70µm, represent additional opportunities to further increase the conversion efficiency. Accordingly, the results presented in this paper show the potential of large-area screen-printed PERC solar cells to achieve conversion efficiencies exceeding 20%.

Acknowledgements

We would like to thank our colleagues at ISFH for fruitful discussions and support in solar cell processing, as well as Heraeus and Ferro for providing the screen-printing pastes. Parts of this work were funded by the German Federal Ministry for the Environment, Nature Conservation and Nuclear Safety under Contract No. 0327529A.

References

[1] International Technology Roadmap for Photovoltaics (ITRPV. net), Results 2010 [available online at http://www.itrpv.net/doc/roadmap_itrpv_2011_brochure_web.pdf], March 2011, p. 15.

[2] Narasimha, S. & Rohatgi, A. 1997, "Optimized aluminum back surface field techniques for silicon solar cells", *Proc. 26th IEEE PVSC*, Anaheim, USA, pp. 63–66.

[3] Peters, S. 2004, "Rapid thermal processing of crystalline silicon materials and solar cells", Ph.D. thesis, University of Konstanz,

Germany, p. 62.
[4] Lorenz, A. et al. 2010, "Influence of surface conditioning and passivation schemes on the internal rear reflectance of bulk silicon solar cells", *Proc. 25th EU PVSEC*, Valencia, Spain, pp. 2059–2061.
[5] Galiazzo, M. et al. 2010, "Double printing of front contact Ag in c-Si solar cells", *Proc. 25th EU PVSEC*, Valencia, Spain, pp. 2338–2340.
[6] Pham, T. et al. 2010, "Improving electrical performance by double print method and non-contact busbars", *Proc. 25th EU PVSEC*, Valencia, Spain, pp. 2378–2380.
[7] Falcon, T. 2010, "High accuracy, high aspect ratio metallization on silicon solar cells using a print on print process", *Proc. 25th EU PVSEC*, Valencia, Spain, pp. 1651–1655.
[8] Blakers, A.W. et al. 1989, "22.8% efficient silicon solar cell", *Appl. Phys. Lett.*, Vol. 55, pp. 1363–1365.
[9] Schmidt, J., Kerr, M. & Cuevas, A. 2001, "Surface passivation of silicon solar cells using plasma-enhanced chemical-vapor-deposited SiN films and thin thermal SiO_2/plasma SiN stacks", *Semicond. Sci. Technol.*, Vol. 16, p. 164.
[10] Hoffmann, M. et al. 2007, "Firing stable surface passivation using all-PECVD stacks of SiO_x:H and SiN_x:H", *Proc. 22nd EU PVSEC*, Milano, Italy, pp. 1030–1033.
[11] Martín, I. et al. 2001, "Surface passivation of p-type crystalline Si by plasma enhanced chemical vapor deposited amorphous SiC_x:H films", *Appl. Phys. Lett.*, Vol. 79, pp. 2199–2201.
[12] Schmidt, J. et al. 2008, "Surface passivation of high-efficiency silicon solar cells by atomic-layer-deposited Al_2O_3", *Prog. in Photovolt.*, Vol. 16, pp. 461–466.
[13] Sperlich, H.-P. et al. 2010, "High productive solar cell passivation on Roth&Rau MAiA® MW-PECVD inline machine – a comparison of Al_2O_3, SiO_2 and SiN_x-H process conditions and performance", *Proc. 25th EU PVSEC*, Valencia, Spain, pp. 1352–1357.
[14] Sunways AG press release, March 2010 [available online at http://www.sunways.eu/en/company/press].
[15] Münzer, K.A. et al. 2010, "Advanced rear side technology for industrial high efficiency solar cells", *Proc. 25th EU PVSEC*, Valencia, Spain, pp. 2314–2318.
[16] Gatz, S. et al. 2011, "19.4%-efficient large-area fully screen-printed silicon solar cells", *Phys. Status Solidi RRL*, Vol. 5, pp. 147–149.
[17] Bosch Solar Energy AG press release, April 2011 [available online at http://www.bosch-solarenergy.com/media-service/press-releases/].
[18] Böscke, T. et al. 2011, "Fully screen-printed PERC cells with laser-fired contacts – an industrial cell concept with 19.5% efficiency", *Proc. 37th IEEE PVSC*, Seattle, USA [in press].
[19] Lai, J.-H. et al. 2011, "Large area 19.6% efficient rear passivated silicon solar cells with local Al BSF and screen-printed contacts", *Proc. 37th IEEE PVSC*, Seattle, USA [in press].
[20] Schmidt, J., Veith, B. & Brendel, R. 2009, "Effective surface passivation of crystalline silicon using ultrathin Al_2O_3 films and Al_2O_3/SiN_x stacks", *Phys. Status Solidi RRL*, Vol. 3, pp. 287–289.
[21] Kerr, M.J. et al. 2001, "Surface recombination velocity of phosphorus-diffused silicon solar cell emitters passivated with plasma enhanced chemical vapor deposited silicon nitride and thermal silicon oxide", *J. Appl. Phys.*, Vol. 89, pp. 3821–3826.
[22] Müller, J. et al. 2011, "Recombination at local aluminum-alloyed silicon solar cell base contacts by dynamic infrared lifetime mapping", *Proc. 1st SiliconPV Conf.*, Freiburg, Germany [in press].
[23] Gatz, S. et al. 2011, "Analysis of local Al-doped back surface fields for high efficiency screen-printed solar cells", *Proc. 1st SiliconPV Conf.*, Freiburg, Germany [in press].
[24] Herguth, A. et al. 2006, "Avoiding boron-oxygen related degradation in highly boron doped Cz silicon", *Proc. 21st EU PVSEC*, Dresden, Germany, pp. 530–537.
[25] Lim, B., Bothe, K. & Schmidt, J. 2008, "Deactivation of the boron–oxygen recombination center in silicon by illumination at elevated temperature", *Phys. Status Solidi RRL*, Vol. 2, pp. 93–95.
[26] Gatz, S., Dullweber, T. & Brendel, R. 2011, "Contact resistance of local rear side contacts of screen-printed silicon PERC solar cells with efficiencies up to 19.4%", *Proc. 37th IEEE PVSC*, Seattle, USA [in press].

About the Authors

Thorsten Dullweber received his Ph.D. from the University of Stuttgart, Germany, in 2002. From 2001 to 2009 he worked as a project leader at Siemens, Infineon and Qimonda. Since 2009 he has led the Solar Cell Production Processes Group in R&D at ISFH, which focuses on process and efficiency improvements of industrial-type silicon solar cells.

Sebastian Gatz has studied in Regensburg, Dublin and Munich. He received his physics diploma from the Technical University of Munich, where he specialized in aluminium-induced crystallization of silicon-germanium for photovoltaic applications. Since 2007 he has been a Ph.D. candidate at ISFH, carrying out research on front- and rear-side-passivated screen-printed solar cells.

Helge Hannebauer studied technical physics at the Leibniz University of Hanover from 2005 to 2009. For his diploma thesis at ISFH he investigated the optimization of screen-printed solar cells. In 2010 he started a Ph.D. program at ISFH, focusing on advanced screen printing and selective emitters.

Tom Falcon has been with DEK since 2001, initially specializing in process development for DEK's Semiconductor Packaging Technologies Team, before moving to DEK Solar in 2008. He is currently responsible for developing metallization processes for silicon solar cells. Prior to joining DEK he held senior engineering positions with IBM, Nortel and Cookson Electronics.

Enquiries

Thorsten Dullweber
Tel: +49 5151 999 638
Fax: +49 5151 999 400
Email: t.dullweber@isfh.de